

Signed Graph Metric Learning via Gershgorin Disc Alignment

Cheng Yang, *Member, IEEE*, Gene Cheung, *Senior Member, IEEE*, Wei Hu, *Member, IEEE*

Abstract—Given a convex and differentiable objective $Q(\mathbf{M})$ for a real, symmetric matrix \mathbf{M} in the positive definite (PD) cone—used to compute Mahalanobis distances—we propose a fast general metric learning framework that is entirely projection-free. We first assume that \mathbf{M} resides in a space \mathcal{S} of generalized graph Laplacian matrices corresponding to balanced signed graphs. $\mathbf{M} \in \mathcal{S}$ that is also PD is called a graph metric matrix. Unlike low-rank metric matrices common in the literature, \mathcal{S} includes the important diagonal-only matrices as a special case. The key theorem to circumvent full eigen-decomposition and enable fast metric matrix optimization is Gershgorin disc alignment (GDA): given $\mathbf{M} \in \mathcal{S}$ and diagonal matrix \mathbf{S} , where $S_{ii} = 1/v_i$ and \mathbf{v} is the first eigenvector of \mathbf{M} , we prove that Gershgorin disc left-ends of similar transform $\mathbf{B} = \mathbf{S}\mathbf{M}\mathbf{S}^{-1}$ are perfectly aligned at the smallest eigenvalue λ_{\min} . Using this theorem, we replace the PD cone constraint in the metric learning problem with tightest possible linear constraints per iteration, so that the alternating optimization of the diagonal / off-diagonal terms in \mathbf{M} can be solved efficiently as linear programs via the Frank-Wolfe method. We update \mathbf{v} using Locally Optimal Block Preconditioned Conjugate Gradient (LOBPCG) with warm start as matrix entries in \mathbf{M} are optimized successively. Experiments show that our graph metric optimization is significantly faster than cone-projection methods, and produces competitive binary classification performance.

Index Terms—Graph signal processing, metric learning, Gershgorin circle theorem, convex optimization

1 INTRODUCTION

The notion of *feature distance* δ_{ij} between two data samples i and j , associated with respective feature vectors $\mathbf{f}_i, \mathbf{f}_j \in \mathbb{R}^K$, is vital for many machine learning applications such as classification [1]. Feature distance is traditionally computed as the *Mahalanobis distance* [2] $\delta_{ij} = (\mathbf{f}_i - \mathbf{f}_j)^\top \mathbf{M} (\mathbf{f}_i - \mathbf{f}_j)$, where $\mathbf{M} \in \mathbb{R}^{K \times K}$ is a *metric matrix* assumed to be positive definite (PD), *i.e.*, $\mathbf{M} \succ 0$ [3]. How to determine the best \mathbf{M} given an objective function $Q(\mathbf{M})$ —*i.e.*, $\min_{\mathbf{M} \succ 0} Q(\mathbf{M})$ —is the *metric learning* problem. We study this basic optimization problem in this paper.

Cheng Yang and Gene Cheung are with York University, Toronto M3J 1P3, ON, Canada (e-mails: cheng.yang@ieee.org, genec@yorku.ca).

Wei Hu is with Peking University, Beijing 100871, China (e-mail: forhuwei@pku.edu.cn).

Corresponding authors: Gene Cheung and Wei Hu.

Gene Cheung acknowledges the support of the NSERC grants [RGPIN-2019-06271], [RGPAS-2019-00110].

Wei Hu acknowledges the support of National Natural Science Foundation of China (61972009) and Beijing Natural Science Foundation (4194080).

There is extensive prior work on the metric learning topic [4], [1], [5]. One fundamental challenge in metric learning is to satisfy the PD cone constraint $\mathbf{M} \succ 0$ when minimizing $Q(\mathbf{M})$ in an efficient manner. A conventional approach is alternating gradient-descent / projection (*e.g.*, proximal gradient (PG) [6]), where a descent step α from current solution \mathbf{M}^t at iteration t in the direction of negative gradient $-\nabla Q(\mathbf{M}^t)$ is followed by a projection $\text{Proj}()$ back to the PD cone, *i.e.*, $\mathbf{M}^{t+1} := \text{Proj}(\mathbf{M}^t - \alpha \nabla Q(\mathbf{M}^t))$. However, projection $\text{Proj}()$ typically requires eigen-decomposition of \mathbf{M}^t and hard-thresholding of its eigenvalues per iteration, which had complexity $\mathcal{O}(K^3)$ and thus is expensive.

To avoid eigen-decomposition, recent methods consider alternative search spaces of matrices such as sparse or low-rank matrices to ease optimization [7], [8], [9], [10], [11]. While efficient, the assumed search spaces are often overly restricted and degrade the quality of sought metric matrix \mathbf{M} . For example, low-rank methods assume reducibility of the K available features to a lower dimension, and hence exclude the simple yet important weighted feature metric case where \mathbf{M} is diagonal [12], *i.e.*, $(\mathbf{f}_i - \mathbf{f}_j)^\top \mathbf{M} (\mathbf{f}_i - \mathbf{f}_j) = \sum_k M_{kk} (f_i^k - f_j^k)^2, M_{kk} > 0, \forall k$.

In this paper, we propose a fast, general metric learning framework, capable of optimizing any convex differentiable objective $Q(\mathbf{M})$, that entirely circumvents eigen-decomposition-based projection on the PD cone. Compared to low-rank methods [10], [9], our framework is more inclusive and includes diagonal metric matrices as a special case. Specifically, we first define a search space \mathcal{S} of general graph Laplacian matrices [13], each corresponding to a balanced¹ signed graph. If in addition $\mathbf{M} \succ 0$, then \mathbf{M} is a *graph metric matrix*. In essence, an underlying graph \mathcal{G} corresponding to $\mathbf{M} \in \mathcal{S}$ contains: i) edge weights reflecting pairwise (anti)-correlations among the K features, and ii) self-loops designating relative importance among the features. Our proposed optimization enables fast searches within space \mathcal{S} .

Our theoretical foundation is a linear algebraic theorem called *Gershgorin disc alignment* (GDA): for any matrix $\mathbf{M} \in \mathcal{S}$, Gershgorin disc left-ends of similar

1. Balance for a feature graph means that if a feature i is positively correlated with feature j , and j with k , then i cannot be negatively correlated with k . See Section 3.3 for details.

transform $\mathbf{B} = \mathbf{S}\mathbf{M}\mathbf{S}^{-1}$, where \mathbf{S} is a diagonal matrix with $S_{ii} = 1/v_i$ and \mathbf{v} is the first eigenvector of \mathbf{M} , can be perfectly aligned at the smallest eigenvalue λ_{\min} . Leveraging GDA for fast metric optimization, we replace the PD cone constraint with a set of K *tightest possible*² linear constraints per iteration as follows: i) compute scalars $S_{ii} = 1/v_i$ from first eigenvector \mathbf{v} of previous solution \mathbf{M}^t , ii) write K linear constraints for K rows of the next solution \mathbf{M}^{t+1} using computed scalars S_{ii} to ensure PDness of \mathbf{M}^{t+1} via the Gershgorin Circle Theorem (GCT) [14]. Linear constraints mean that our proposed alternating optimization of the diagonal / off-diagonal terms in \mathbf{M}^{t+1} can be solved speedily as linear programs (LP) [15] via the Frank-Wolfe method [16].

The bulk of the algorithm complexity resides in the repeated computation of the first eigenvectors \mathbf{v} of \mathbf{M}^t . We update \mathbf{v} using *Locally Optimal Block Preconditioned Conjugate Gradient* (LOBPCG) [17] with warm start as diagonal / off-diagonal terms are optimized successively. Extensive experiments show that our graph metric optimization is significantly faster than cone-projection methods (up to 5x speedup for large K), and produces competitive binary classification performance.

The paper is organized as follows. We first review previous works in Section 2. We describe GDA in Section 3. Leveraging GDA, we describe our metric optimization framework in Section 4 and 5. Finally, experiments and conclusions are presented in Section 6 and 7, respectively.

2 RELATED WORK

We divide existing methods into two main categories: linear and nonlinear distance metric learning.

2.1 Linear Distance Metric Learning

These methods learn linear transformations to project samples into a new feature space. This paradigm is prevalent in the metric learning community, as many of the resulting transformations are tractable. Mahalanobis distance metric is one representative linear metric, which has been extensively studied under a variety of assumptions. Some methods assume that the desired metric \mathbf{M} inherently lies in a lower dimension than the original K -dimensional feature space, and utilize projections such as Principle Component Analysis (PCA) [1] and random projection [18]. However, the employed projections can be computationally expensive, while yielding sub-optimal solutions due to reduced dimensionality. Some methods make structural assumptions on the sought metric matrix to ease optimization, such as low rank [9], [10] and sparsity [7], [8]. For example, Liu *et al.* propose convex and low-rank metric learning, which decomposes the learning task into two steps: an SVD-based projection and a metric learning problem with reduced dimensionality [9]. Other assumptions enforce the

2. By “tightest possible”, we mean that the lower bound $\lambda_{\min}^-(\mathbf{B})$ of the smallest eigenvalue $\lambda_{\min}(\mathbf{B})$ —smallest Gershgorin disc left-end of matrix \mathbf{B} —and $\lambda_{\min}(\mathbf{B})$ are the same. See Section 3 for details.

distance metric to be a diagonal matrix [19] or a sparse matrix [7], [8]. However, the structural assumptions of the metric matrix are often too strong, resulting in overly restricted search spaces and sub-optimal metrics.

2.2 Nonlinear Distance Metric Learning

Given possibly nonlinear relationship of data points, these methods learn nonlinear transformations to map samples into another feature space. While kernelized linear transformations can be adopted to address the nonlinearity problem [20], [21], choosing a kernel is typically difficult and empirical, and often not flexible enough to capture the nonlinearity in the data. Given that deep learning is effective in modeling function nonlinearities, deep metric learning (DML) methods employ various deep neural network architectures to learn a set of hierarchical transformations for nonlinear mapping of data points [22]. DML methods mainly include Siamese-networks based methods [23], [24], [25], [26] and triplet-networks based methods [27], [28], [29], [30]. The objective functions are often designed for different specific tasks. DML has shown substantial benefits in wide applications of various visual understanding tasks such as image classification, visual search, visual tracking and so on. However, they are mostly trained in a supervised fashion, requiring a large amount of labeled data.

In contrast, our metric optimization framework does not require bulk training data, and is suitable for any convex and differentiable objective, including proposals in [31], [1], [32], [33]. We are thus agnostic to the question which metric objective is the best; instead, we argue that our general optimization framework can benefit a broad class of metric objectives, requiring only that the cost function $Q(\mathbf{M})$ is convex and differentiable.

2.3 GDA-based Graph Sampling

We have studied Gershgorin disc alignment (GDA) in the context of graph sampling in our previous work [34], [35]. There are two key differences between our current work and [34], [35]: i) we derive theorems to show *perfect* alignment of Gershgorin disc left-ends at λ_{\min} for defined classes of matrices, while alignment in [34], [35] is only approximate; and ii) we employ GDA in a formal optimization framework for metric learning.

Our preliminary work on GDA for metric learning [36] assumes a restricted search space of Laplacian matrices for irreducible *positive* graphs with positive node degrees. Here we generalize to a much larger space of Laplacian matrices for *balanced signed* graphs.

3 GERSHGORIN DISC ALIGNMENT

We first review basic definitions in graph signal processing (GSP) [37] that are necessary to understand our GDA theory. We then describe GDA for positive graphs and balanced signed graphs in order.

3.1 Graph and Graph Laplacian Matrices

We consider an undirected graph $\mathcal{G} = \{\mathcal{N}, \mathcal{E}, \mathcal{U}\}$ containing a node set \mathcal{N} of cardinality $|\mathcal{N}| = K$. Each inter-node edge $(i, j) \in \mathcal{E}$, $i \neq j$, has an associated weight $w_{ij} \in \mathbb{R}$ that reflects the degree of (dis)similarity or (anti-)correlation between nodes i and j , depending on the sign of w_{ij} . Each node i may have a self-loop $(i) \in \mathcal{U}$ with weight $u_i \in \mathbb{R}$.

One can collect edge weights and self-loops into an *adjacency matrix* \mathbf{W} , where $W_{ij} = w_{ij}$, $(i, j) \in \mathcal{E}$, and $W_{ii} = u_i$, $(i) \in \mathcal{U}$. We define $\mathbf{D} = \mathbf{W}1$ as a diagonal *degree matrix* that accounts for both inter-node edges and self-loops (1 is a column vector of all one's). The *combinatorial graph Laplacian matrix* [37] is defined as $\mathbf{L} = \mathbf{D} - \mathbf{W}$. A *generalized graph Laplacian matrix* [13] accounts for self-loops in \mathcal{G} also and is defined as $\mathbf{L}_g = \mathbf{D} - \mathbf{W} + \text{diag}(\mathbf{W})$, where $\text{diag}(\mathbf{W})$ extracts the diagonal entries of \mathbf{W} . Alternatively, we can write $\mathbf{L}_g = \mathbf{D} - \mathbf{W}_g$, where $\mathbf{W}_g = \mathbf{W} - \text{diag}(\mathbf{W})$ contains only inter-node edge weights (diagonal terms are zeros).

3.2 GDA for Positive Graphs

Consider first the simpler case of a *positive graph*, where an irreducible³ graph \mathcal{G} (no disconnected nodes) has strictly positive edge weights and self-loops, *i.e.*, $w_{ij} > 0$, $(i, j) \in \mathcal{E}$ and $u_i > 0$, $(i) \in \mathcal{U}$. This means that \mathbf{W} is non-negative, the diagonals in \mathbf{D} are strictly positive, and the generalized graph Laplacian \mathbf{L}_g is positive semi-definite (PSD) [39]. We discuss first GDA for this case.

3.2.1 Gershgorin Circle Theorem

We first overview *Gershgorin Circle Theorem* (GCT) [14]. By GCT, each real eigenvalue λ of a real symmetric matrix \mathbf{M} resides in at least one *Gershgorin disc* Ψ_i , corresponding to row i of \mathbf{M} , with center $c_i = M_{ii}$ and radius $r_i = \sum_{j \neq i} |M_{ij}|$, *i.e.*,

$$\exists i \text{ s.t. } c_i - r_i \leq \lambda \leq c_i + r_i \quad (1)$$

Thus a sufficient (but not necessary) condition to guarantee that \mathbf{M} is PSD (smallest eigenvalue $\lambda_{\min} \geq 0$) is to ensure that the smallest Gershgorin disc left-end λ_{\min}^- —a lower bound for λ_{\min} —is non-negative, *i.e.*,

$$0 \leq \lambda_{\min}^- = \min_i c_i - r_i \leq \lambda_{\min} \quad (2)$$

However, λ_{\min}^- is often much smaller λ_{\min} , resulting in a loose lower bound. As an illustration, consider the following example 3×3 PD matrix \mathbf{M} :

$$\mathbf{M} = \begin{bmatrix} 2 & -2 & -1 \\ -2 & 5 & -2 \\ -1 & -2 & 4 \end{bmatrix} \quad (3)$$

Lower bound $\lambda_{\min}^- = \min(-1, 1, 1) = -1$, while the smallest eigenvalue for \mathbf{M} is $\lambda_{\min} = 0.1078 > 0$. See Fig. 1 for an illustration of Gershgorin discs for this example.

3. An irreducible graph \mathcal{G} means that there exists a path from any node in \mathcal{G} to any other node in \mathcal{G} [38].

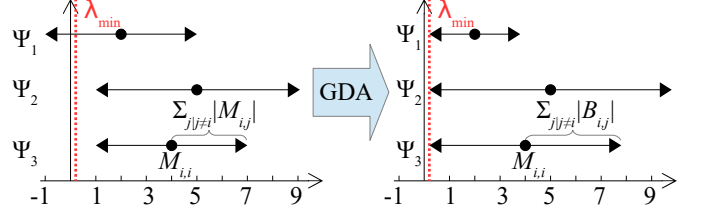


Fig. 1. Illustration of Gershgorin discs for matrix \mathbf{M} in (3) (left), and aligned discs for $\mathbf{B} = \mathbf{S}\mathbf{M}\mathbf{S}^{-1}$ (right).

3.2.2 GDA Analysis for Positive Graphs

GDA is a procedure to scale the Gershgorin disc radii r_i of matrix \mathbf{M} , so that all disc left-ends $c_i - r_i$ are perfectly aligned at $\lambda_{\min}(\mathbf{M})$. In other words, after GDA the GCT lower bound $\lambda_{\min}^-(\mathbf{M})$ for smallest eigenvalue $\lambda_{\min}(\mathbf{M})$ is the *tightest possible*. Specifically, we perform a *similarity transform* [40] of \mathbf{M} via matrix \mathbf{S} , *i.e.*,

$$\mathbf{B} = \mathbf{S}\mathbf{M}\mathbf{S}^{-1} \quad (4)$$

where $\mathbf{S} = \text{diag}(s_1, \dots, s_K)$ is chosen to be a diagonal *scaling matrix* with scalars s_1, \dots, s_K along its diagonal, where $s_i > 0$, $\forall i$. \mathbf{B} has the same eigenvalues as \mathbf{M} , and thus the smallest Gershgorin disc left-end for \mathbf{B} is also a lower bound for \mathbf{M} 's smallest eigenvalue λ_{\min} , *i.e.*,

$$\lambda_{\min}^-(\mathbf{B}) \leq \lambda_{\min}(\mathbf{B}) = \lambda_{\min}(\mathbf{M}) \quad (5)$$

$$= \min_i B_{ii} - \sum_{j \neq i} |B_{ij}| \quad (6)$$

$$= \min_i M_{ii} - s_i \sum_{j \neq i} |M_{ij}|/s_j \quad (7)$$

We show that given a generalized graph Laplacian matrix \mathbf{M} corresponding to an irreducible, positive graph \mathcal{G} , there exist scalars s_1, \dots, s_K such that all Gershgorin disc left-ends of $\mathbf{B} = \mathbf{S}\mathbf{M}\mathbf{S}^{-1}$ are aligned at exactly $\lambda_{\min}(\mathbf{M})$. We state this formally as a theorem.

Theorem 1. *Let \mathbf{M} be a generalized graph Laplacian matrix corresponding to an irreducible, positive graph \mathcal{G} . Denote by \mathbf{v} the first eigenvector of \mathbf{M} corresponding to the smallest eigenvalue λ_{\min} . Then by computing scalars $s_i = 1/v_i$, $\forall i$, all Gershgorin disc left-ends of $\mathbf{B} = \mathbf{S}\mathbf{M}\mathbf{S}^{-1}$, $\mathbf{S} = \text{diag}(s_1, \dots, s_K)$, are aligned at λ_{\min} , *i.e.*, $B_{ii} - \sum_{j \neq i} |B_{ij}| = \lambda_{\min}$, $\forall i$.*

Continuing our earlier example, using $s_1 = 0.7511$, $s_2 = 0.4886$ and $s_3 = 0.4440$, we see that $\mathbf{B} = \mathbf{S}\mathbf{M}\mathbf{S}^{-1}$ for \mathbf{M} in (3) has all disc left-ends aligned at $\lambda_{\min} = 0.1078$.

To prove Theorem 1, we first establish the following lemma.

Lemma 1. *There exists a first eigenvector \mathbf{v} with strictly positive entries for a generalized graph Laplacian matrix \mathbf{M} corresponding to an irreducible, positive graph \mathcal{G} .*

Proof: By definition, \mathbf{M} is a generalized graph Laplacian $\mathbf{M} = \mathbf{D} - \mathbf{W}_g$ with positive inter-node edge weights

in \mathbf{W}_g and positive degrees in \mathbf{D} . Let \mathbf{v} be the first eigenvector of \mathbf{M} , *i.e.*,

$$\begin{aligned}\mathbf{M}\mathbf{v} &= \lambda_{\min}\mathbf{v} \\ (\mathbf{D} - \mathbf{W}_g)\mathbf{v} &= (\lambda_{\min}\mathbf{I})\mathbf{v} \\ \mathbf{D}\mathbf{v} &= (\mathbf{W}_g + \lambda_{\min}\mathbf{I})\mathbf{v} \\ \mathbf{v} &= \mathbf{D}^{-1}(\mathbf{W}_g + \lambda_{\min}\mathbf{I})\mathbf{v}\end{aligned}$$

where \mathbf{I} is an identity matrix, and $\lambda_{\min} \geq 0$ since \mathbf{M} is PSD. Since the matrix on the right contains only non-negative entries and \mathbf{W}_g is an irreducible matrix (graph \mathcal{G} is irreducible), \mathbf{v} is a positive eigenvector by the Perron-Frobenius Theorem [41]. \square

We now prove Theorem 1 as follows.

Proof: Denote by \mathbf{v} a strictly positive eigenvector corresponding to the smallest eigenvalue λ_{\min} of \mathbf{M} . Define $\mathbf{S} = \text{diag}(1/v_1, \dots, 1/v_K)$. Then,

$$\mathbf{S}\mathbf{M}\mathbf{S}^{-1}\mathbf{S}\mathbf{v} = \lambda_{\min}\mathbf{S}\mathbf{v} \quad (8)$$

where $\mathbf{S}\mathbf{v} = \mathbf{1} = [1, \dots, 1]^\top$. Let $\mathbf{B} = \mathbf{S}\mathbf{M}\mathbf{S}^{-1}$. Then,

$$\mathbf{B}\mathbf{1} = \lambda_{\min}\mathbf{1} \quad (9)$$

(9) means that

$$B_{ii} + \sum_{j|j \neq i} B_{ij} = \lambda_{\min}, \quad \forall i$$

Note that the off-diagonal terms $B_{ij} = (v_i/v_j)M_{ij} \leq 0$, since: i) \mathbf{v} is strictly positive, and ii) off-diagonal terms of generalized graph Laplacian \mathbf{M} for a positive graph satisfy $M_{i,j} \leq 0$. Thus,

$$B_{ii} - \sum_{j|j \neq i} |B_{ij}| = \lambda_{\min}, \quad \forall i \quad (10)$$

Thus, defining $\mathbf{S} = \text{diag}(1/v_1, \dots, 1/v_K)$ means that $\mathbf{B} = \mathbf{S}\mathbf{M}\mathbf{S}^{-1}$ has all its Gershgorin disc left-ends aligned at λ_{\min} . \square

3.3 GDA for Balanced Signed Graphs

We generalize our GDA analysis to signed graphs, where weights for edges and self-loops can be negative. Central to our analysis is the concept of *graph balance*. We first discuss graph balance and the related Cartwright-Harary Theorem (CHT) [42], then present our GDA analysis.

3.3.1 Cartwright-Harary Theorem

The concept of balance in a signed graph has been studied in many scientific disciplines, including psychology, social networks and data mining [43]. We adopt the following definition of a balance graph for our analysis:

Definition 1. A signed graph \mathcal{G} is balanced if \mathcal{G} does not contain any cycle with odd number of negative edges.

For intuition, consider a graph \mathcal{G} with three nodes denoted by A , B and C . Suppose that a positive/negative edge reflects pairwise friend/enemy relationship. An edge assignment of $(A, B) = 1$ and $(B, C) = (C, A) = -1$ —resulting in a cycle of two negative edges—means

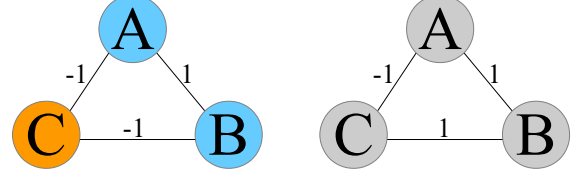


Fig. 2. Examples of a 3-node balanced signed graph (left) and an unbalanced signed graph (right).

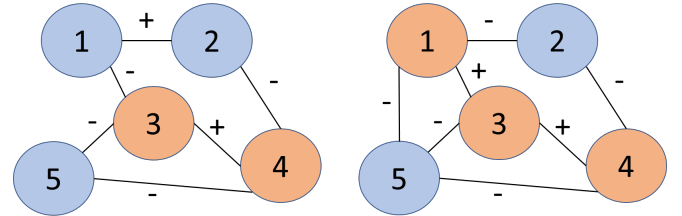


Fig. 3. Example of two 5-node balanced graphs. Node 1 has turned from blue to red from the left to the right.

that A and B are friends, and that both A and B are enemies with C . See Fig. 2 for an illustration. This graph is balanced; entities can be grouped into *two* clusters, $\{A, B\}$ and $\{C\}$, where entities within a cluster are friends, and entities across clusters are enemies.

In contrast, an edge assignment of $(A, B) = (B, C) = 1$ and $(C, A) = -1$ —resulting in a cycle of one negative edge—means that both A and C are friends with B , but A and C are enemies. This graph is not balanced; one cannot assign entities to two distinct clusters with consistent signs as we did previously. We can generalize this example to the CHT [42] as follows.

Theorem 2. A graph \mathcal{G} is balanced iff its nodes \mathcal{N} can be partitioned into blue and red clusters, \mathcal{N}_b and \mathcal{N}_r , such that a positive edge always connects two same-color nodes, and a negative edge always connects two opposite-color nodes.

There are two implications. First, to determine if graph \mathcal{G} is balanced, instead of examining all cycles in \mathcal{G} and checking if each contains an odd number of negative edges, one can check if nodes can be colored into blue and red with consistent edge signs as stated in Theorem 2. Second, we can use CHT to prove that GDA is possible for a Laplacian matrix corresponding to an irreducible, balanced signed graph. We describe this next.

3.3.2 GDA Analysis for Signed Graphs

Consider an irreducible, balanced signed graph $\mathcal{G}(\mathcal{N}, \mathcal{E}^+ \cup \mathcal{E}^-, \mathcal{U})$ with nodes \mathcal{N} , positive and negative inter-node edges, \mathcal{E}^+ and \mathcal{E}^- , and self-loops \mathcal{U} . According to CHT, nodes \mathcal{N} can be partitioned into blue and red clusters, \mathcal{N}_b and \mathcal{N}_r , such that

- 1) $(i, j) \in \mathcal{E}^+$ implies that either $i, j \in \mathcal{N}_b$ or $i, j \in \mathcal{N}_r$.
- 2) $(i, j) \in \mathcal{E}^-$ implies that either $i \in \mathcal{N}_b$ and $j \in \mathcal{N}_r$, or $i \in \mathcal{N}_r$ and $j \in \mathcal{N}_b$.

As an example, consider the 5-node balanced graph in Fig. 3(left), where nodes 1, 2 and 5 are colored blue, while nodes 3 and 4 are colored red. Only positive edges connect same-color node pairs, while negative edges connect opposite-color node pairs. There is no cycle of odd number of negative edges.

We now state a generalization of Theorem 1 to balanced signed graphs as follows:

Theorem 3. Denote by \mathbf{M} a generalized graph Laplacian matrix corresponding to a balanced, irreducible signed graph \mathcal{G} . Denote by \mathbf{v} the first eigenvector of \mathbf{M} corresponding to the smallest eigenvalue λ_{\min} . Define $\mathbf{B} = \mathbf{S}\mathbf{M}\mathbf{S}^{-1}$ as a similarity transform of \mathbf{M} , where $\mathbf{S} = \text{diag}(s_1, \dots, s_K)$. If $s_i = 1/v_i$, where $v_i \neq 0, \forall i$, then Gershgorin disc left-ends of \mathbf{B} are aligned at λ_{\min} , i.e., $B_{ii} - \sum_{j|j \neq i} |B_{ij}| = \lambda_{\min}, \forall i$.

We prove Theorem 3 as follows.

Proof: We first reorder blue nodes before red nodes in the rows and columns of \mathbf{M} , so that \mathbf{M} can be written as a 2×2 block matrix as follows:

$$\mathbf{M} = \begin{bmatrix} \mathbf{M}_{11} & \mathbf{M}_{12} \\ \mathbf{M}_{12}^\top & \mathbf{M}_{22} \end{bmatrix} \quad (11)$$

where off-diagonal terms in \mathbf{M}_{11} (\mathbf{M}_{22}) are negative stemming from positive edge weights $w_{ij} \geq 0$ connecting same-color nodes, and entries in \mathbf{M}_{12} are positive stemming from negative edge weights $w_{ij} \leq 0$ connecting different-color nodes. Define now a similarity transform \mathbf{M}' of \mathbf{M} :

$$\mathbf{M}' = \begin{bmatrix} \mathbf{I}_b & \mathbf{0} \\ \mathbf{0} & -\mathbf{I}_r \end{bmatrix} \begin{bmatrix} \mathbf{M}_{11} & \mathbf{M}_{12} \\ \mathbf{M}_{12}^\top & \mathbf{M}_{22} \end{bmatrix} \begin{bmatrix} \mathbf{I}_b & \mathbf{0} \\ \mathbf{0} & -\mathbf{I}_r \end{bmatrix} \quad (12)$$

$$= \begin{bmatrix} \mathbf{M}_{11} & -\mathbf{M}_{12} \\ -\mathbf{M}_{12}^\top & \mathbf{M}_{22} \end{bmatrix} \quad (13)$$

We interpret $\mathbf{M}' = \mathbf{D} - \mathbf{W}'_g$ as a generalized graph Laplacian matrix for a new graph $\mathcal{G}'(\mathcal{N}, \mathcal{E}', \mathcal{U}')$ derived from \mathcal{G} , where \mathcal{G}' retains positive edges \mathcal{E}^+ , but for each negative edge \mathcal{E}^- , \mathcal{G}' switches its sign to positive. Thus,

$$w'_{ij} = \begin{cases} w_{ij} & \text{if } (i, j) \in \mathcal{E}^+ \\ -w_{ij} & \text{if } (i, j) \in \mathcal{E}^- \end{cases} \quad (14)$$

To retain the same degree matrix \mathbf{D} as \mathcal{G} , we assign a self-loop for each node i in \mathcal{G}' with weight u'_i defined as

$$u'_i = u_i + 2 \sum_{j|j \neq i} w_{ij} \quad (15)$$

As a similarity transform, \mathbf{M} and \mathbf{M}' have the same eigenvalues, and an eigenvector \mathbf{z} for \mathbf{M}' maps to an eigenvector \mathbf{v} for \mathbf{M} as follows:

$$\mathbf{v} = \begin{bmatrix} \mathbf{I}_b & \mathbf{0} \\ \mathbf{0} & -\mathbf{I}_r \end{bmatrix} \mathbf{z} \quad (16)$$

Finally, we define a *shifted* graph Laplacian matrix $\mathbf{M}'' = \mathbf{M}' + \epsilon \mathbf{I}$, where constant $\epsilon > 0$ is

$$\epsilon > \max_i \left\{ - \sum_{j|j \neq i} w_{ij} - u_i \right\} \quad (17)$$

\mathbf{M}'' has the same set of eigenvectors as \mathbf{M}' , and its eigenvalues are the same as \mathbf{M}' but offset by ϵ .

\mathbf{M}'' has strictly positive node degrees D''_{ii} , i.e.,

$$\begin{aligned} D''_{ii} &= \sum_{j|j \neq i} w'_{ij} + u'_i + \epsilon \\ &= \sum_{j|j \neq i} w_{ij} - \sum_{j|j \neq i} w_{ij} + u_i + 2 \sum_{j|j \neq i} w_{ij} + \epsilon \\ &= \sum_{j|j \neq i} w_{ij} + \sum_{j|j \neq i} w_{ij} + u_i + \epsilon \stackrel{(a)}{>} 0 \end{aligned}$$

(a) is due to the assumed inequality for ϵ in (17).

From Theorem 1, given \mathbf{M}'' is a Laplacian matrix for an irreducible positive graph, first eigenvector of \mathbf{M}'' (also first eigenvector of \mathbf{M}') \mathbf{z} is a strictly positive vector. Thus, from (16), corresponding \mathbf{v} for \mathbf{M} is a strictly non-zero first eigenvector, i.e., $v_i \neq 0, \forall i$.

Having established first eigenvector \mathbf{v} of \mathbf{M} , we define diagonal matrix $\mathbf{S} = \text{diag}(1/v_1, \dots, 1/v_N)$, and write

$$\mathbf{S}\mathbf{M}\mathbf{S}^{-1}\mathbf{S}\mathbf{v} = \lambda_{\min}\mathbf{S}\mathbf{v} \quad (18)$$

$$\mathbf{B}\mathbf{1} = \lambda_{\min}\mathbf{1} \quad (19)$$

where $\mathbf{B} = \mathbf{S}\mathbf{M}\mathbf{S}^{-1}$. Each row i in (19) states that

$$B_{ii} + \sum_{j|j \neq i} B_{ij} = \lambda_{\min} \quad (20)$$

$$M_{ii} + s_i \sum_{j|j \neq i} M_{ij}/s_j = \lambda_{\min} \quad (21)$$

Suppose i is a red node. Then $v_i = -z_i < 0$, and thus $s_i = 1/v_i < 0$. For each red neighbor j of i , $s_j < 0$, and $w_{ij} > 0$ means that $M_{ij} < 0$. We can hence conclude that $s_i M_{ij}/s_j < 0$ and $s_i M_{ij}/s_j = -|s_i M_{ij}/s_j|$. For each blue neighbor j of i , $s_j > 0$, and $w_{ij} < 0$ means that $M_{ij} > 0$. We can hence conclude also that $s_i M_{ij}/s_j < 0$ and $s_i M_{ij}/s_j = -|s_i M_{ij}/s_j|$. Similar analysis can be performed if i is a blue node. Thus (21) can be rewritten as

$$M_{ii} - \sum_{j|j \neq i} |s_i M_{ij}/s_j| = \lambda_{\min} \quad (22)$$

In other words, the left-end of \mathbf{B} 's i -th Gershgorin disc—centre M_{ii} minus radius $\sum_{j|j \neq i} |s_i M_{ij}/s_j|$ —is aligned at λ_{\min} . This holds true for all i . \square

4 OPTIMIZING METRIC DIAGONALS

We now use GDA to optimize a metric matrix \mathbf{M} . We first define our search space of metric matrices and our problem to optimize \mathbf{M} 's diagonal terms. We then describe how GDA can be used in combination with the Frank-Wolfe method to speed up our optimization.

4.1 Search Space of Graph Metric Matrices

We assume that associated with each data sample i is a length- K feature vector $\mathbf{f}_i \in \mathbb{R}^K$. A *metric matrix*

$\mathbf{M} \in \mathbb{R}^{K \times K}$ defines the feature distance $\delta_{ij}(\mathbf{M})$ —the *Mahalanobis distance* [2]—between samples i and j as:

$$\delta_{ij}(\mathbf{M}) = (\mathbf{f}_i - \mathbf{f}_j)^\top \mathbf{M} (\mathbf{f}_i - \mathbf{f}_j) \quad (23)$$

By definition of a metric [3], one requires \mathbf{M} to be a *positive definite* (PD) matrix, denoted by $\mathbf{M} \succ 0$. This means that $\delta_{ij}(\mathbf{M})$ is strictly positive unless $\mathbf{f}_i = \mathbf{f}_j$, *i.e.*, $(\mathbf{f}_i - \mathbf{f}_j)^\top \mathbf{M} (\mathbf{f}_i - \mathbf{f}_j) > 0$ if $\mathbf{f}_i - \mathbf{f}_j \neq 0$.

To efficiently enforce $\mathbf{M} \succ 0$, we invoke our developed GDA theory that involves generalized graph Laplacian matrices. We define the search space \mathcal{S} of matrices for our optimization framework as follows:

Definition 2. \mathcal{S} is a space of real, symmetric matrices that are generalized graph Laplacian matrices corresponding to irreducible, balanced signed graphs.

We call a matrix $\mathbf{M} \in \mathcal{S}$ that is also PD, denoted by $\mathbf{M} \succ 0$, a *graph metric matrix*.

4.2 Problem Formulation

We pose an optimization problem for \mathbf{M} : find an optimal graph metric \mathbf{M} —leading to feature distances $\delta_{ij}(\mathbf{M})$ in (23)—that yields the smallest value of a convex differentiable objective $Q(\{\delta_{ij}(\mathbf{M})\})$, *i.e.*,

$$\min_{\mathbf{M} \in \mathcal{S}} Q(\{\delta_{ij}(\mathbf{M})\}), \quad \text{s.t. } \begin{cases} \text{tr}(\mathbf{M}) \leq C \\ \mathbf{M} \succ 0 \end{cases} \quad (24)$$

where $C > 0$ is a chosen parameter. Constraint $\text{tr}(\mathbf{M}) \leq C$ is needed to avoid pathological solutions with infinite feature distances, *i.e.*, $\delta_{ij}(\mathbf{M}) = \infty$. For stability, we assume also that the objective is lower-bounded, *i.e.*, $\min_{\mathbf{M} \succ 0} Q(\{\delta_{ij}(\mathbf{M})\}) \geq \kappa > -\infty$ for some constant κ . We examine examples of objective $Q(\{\delta_{ij}(\mathbf{M})\})$ in Section 6.

Our strategy to solve (24) is to optimize \mathbf{M} 's diagonal terms *plus* one row/column of off-diagonal terms at a time using the Frank-Wolfe (FW) iterative method [16], where each FW iteration is solved as an LP until convergence. We discuss first the initialization of \mathbf{M} , then the optimization setup for \mathbf{M} 's diagonal terms. For notation convenience, we will write the objective simply as $Q(\mathbf{M})$, with the understanding that metric \mathbf{M} computes first the feature distances $\delta_{ij}(\mathbf{M})$, which in turn determines the objective $Q(\{\delta_{ij}(\mathbf{M})\})$.

4.2.1 Initialization of Metric \mathbf{M}

We first initialize a valid graph metric \mathbf{M}^0 as follows:

- 1) Initialize each diagonal term $M_{ii}^0 := C/K$.
- 2) Initialize off-diagonal terms $M_{ij}^0, i \neq j$, as:

$$M_{ij}^0 := \begin{cases} \epsilon (-1)^{\min(i,j)} & \text{if } j = i \pm 1 \\ 0 & \text{o.w.} \end{cases} \quad (25)$$

where $\epsilon > 0$ is a small parameter. Initialization of the diagonal terms ensures that constraint $\text{tr}(\mathbf{M}^0) \leq C$ is satisfied. Initialization of the off-diagonal terms ensures that \mathbf{M}^0 is symmetric and PD ($C/K - 2|\epsilon| > 0$), and that the underlying graph \mathcal{G} is a chain with nodes connected by edges of alternating signs. Because \mathcal{G} is a chain graph,

it is always balanced. We can hence conclude that initial \mathbf{M}^0 is a graph metric, *i.e.*, $\mathbf{M}^0 \in \mathcal{S}$ and $\mathbf{M}^0 \succ 0$.

4.2.2 Optimization of Diagonals

Optimizing \mathbf{M} 's diagonal terms M_{ii} alone, (24) becomes

$$\begin{aligned} \min_{\{M_{ii}\}} \quad & Q(\mathbf{M}) \\ \text{s.t.} \quad & \mathbf{M} \succ 0; \quad \sum_i M_{ii} \leq C; \quad M_{ii} > 0, \forall i \end{aligned} \quad (26)$$

where $\text{tr}(\mathbf{M}) = \sum_i M_{ii}$. Because the diagonal terms do not affect the irreducibility and balance of matrix \mathbf{M} , the only requirement for \mathbf{M} to be a graph metric is just to ensure \mathbf{M} is PD.

4.3 Replacing PD Cone with GDA Linear Constraints

To efficiently enforce $\mathbf{M} \succ 0$, we derive sufficient (but not necessary) linear constraints using GCT [14]. A direct application of GCT on \mathbf{M} , as discussed in Section 3.2.1, translates to a linear constraint for each row i :

$$M_{ii} \geq \sum_{j \mid j \neq i} |M_{ij}| + \rho, \quad \forall i \in \{1, \dots, K\} \quad (27)$$

where $\rho > 0$ is a small parameter.

However, as discussed in Section 3.2.1, GCT lower bound $\lambda_{\min}^- = \min_i M_{ii} - \sum_{j \neq i} |M_{ij}|$ for λ_{\min} can be loose. When optimizing \mathbf{M} , enforcing (27) directly can mean a severely restricted space compared to the original $\{\mathbf{M} \mid \mathbf{M} \succ 0\}$ in (26), resulting in an inferior solution.

To derive more appropriate linear constraints—thus a more comparable search space to original $\{\mathbf{M} \mid \mathbf{M} \succ 0\}$ when solving $\min Q(\mathbf{M})$ —we leverage our GDA theory and examine instead the Gershgorin discs of a similarity-transformed matrix \mathbf{B} from \mathbf{M} , *i.e.*, $\mathbf{B} = \mathbf{S}\mathbf{M}\mathbf{S}^{-1}$, where $\mathbf{S} = \text{diag}(s_1, \dots, s_K)$. This leads to the following linear constraints instead:

$$M_{ii} \geq \sum_{j \mid j \neq i} \left| \frac{s_i M_{ij}}{s_j} \right| + \rho, \quad \forall i \in \{1, \dots, K\} \quad (28)$$

The crux is in the selection of scalars s_i . Suppose that the optimal solution \mathbf{M}^* to (26) is known. Then, using the first eigenvector \mathbf{v}^* of \mathbf{M}^* corresponding to the smallest eigenvalue $\lambda_{\min}^* > 0$, one can compute $s_i = 1/v_i^*$ to define linear constraints (28). By Theorem 3, disc left-ends of $\mathbf{B} = \mathbf{S}\mathbf{M}^*\mathbf{S}^{-1}$ are aligned exactly at λ_{\min}^* , and thus \mathbf{M}^* is a feasible solution to (28). Linear constraints (28) are *tightest possible* for solution \mathbf{M}^* , in the sense that $\lambda_{\min}^-(\mathbf{B}) = \lambda_{\min}(\mathbf{B}) = \lambda_{\min}(\mathbf{M}^*)$.

Of course, in practice we do not have solution \mathbf{M}^* available *a priori* to compute \mathbf{v}^* . Thus, we solve the optimization iteratively, where we use the previous solution \mathbf{M}^t at iteration t to compute scalars s_i^t 's, solve for a better solution \mathbf{M}^{t+1} using linear constraints (28), compute new scalars again etc until convergence. Specifically,

- 1) Given scalars s_i^t 's, identify a good solution \mathbf{M}^{t+1}

minimizing objective $Q(\mathbf{M})$ subject to (28), *i.e.*,

$$\begin{aligned} \min_{\{M_{ii}\}} & Q(\mathbf{M}) \\ \text{s.t. } & M_{ii} \geq \sum_{j \mid j \neq i} \left| \frac{s_i^t M_{ij}}{s_j^t} \right| + \rho, \forall i; \quad \sum_i M_{ii} \leq C \end{aligned} \quad (29)$$

- 2) Given computed \mathbf{M}^{t+1} , update scalars $s_i^{t+1} = 1/v_i^{t+1}$ where \mathbf{v}^{t+1} is the first eigenvector of \mathbf{M}^{t+1} .
- 3) Increment t and repeat until convergence.

When the scalars in (29) are updated as $s_i^{t+1} = 1/v_i^{t+1}$, previously computed \mathbf{M}^{t+1} still satisfies linear constraints in (29) in the next iteration, which means that the objective $Q(\mathbf{M}^t)$ is non-increasing across iterations. Given that $Q(\mathbf{M})$ is decreasing and is lower-bounded by κ by assumption, we conclude that the loop converges to a local optimal solution where $\mathbf{M}^{t+1} = \mathbf{M}^t$.

The remaining issue is how to best compute first eigenvector \mathbf{v}^{t+1} given solution \mathbf{M}^{t+1} repeatedly. For this task, we employ *Locally Optimal Block Preconditioned Conjugate Gradient* (LOBPCG) [17], a fast algorithm known to compute extreme eigenpairs efficiently, with complexity $O(ab)$, where a denotes the number of non-zero entries in \mathbf{M} and b denotes the number of iterations till convergence in LOBPCG. Because LOBPCG is itself iterative, it benefits from *warm start*: algorithm converges much faster if a good solution initiates the iterations. In our case, we use previously computed eigenvector \mathbf{v}^t as an initial solution to speed up LOBPCG when computing \mathbf{v}^{t+1} , reducing its complexity substantially.

4.4 Frank-Wolfe Method

4.4.1 FW Step 1: Solving LP

To solve (29), we employ the Frank-Wolfe (FW) method [16]. The first FW step linearizes the objective $Q(\mathbf{M})$ using its gradient $\nabla Q(\mathbf{M}^t)$ with respect to diagonal terms $\{M_{ii}\}$, computed using previous solution \mathbf{M}^t , *i.e.*,

$$\nabla Q(\mathbf{M}^t) = \left[\begin{array}{c} \frac{\partial Q(\mathbf{M})}{\partial M_{1,1}} \\ \vdots \\ \frac{\partial Q(\mathbf{M})}{\partial M_{K,K}} \end{array} \right] \Big|_{\mathbf{M}^t} \quad (30)$$

Given gradient $\nabla Q(\mathbf{M}^t)$, optimization (29) becomes a *linear program* (LP) at each iteration t :

$$\begin{aligned} \min_{\{M_{ii}\}} & \text{vec}(\{M_{ii}\})^\top \nabla Q(\mathbf{M}^t) \\ \text{s.t. } & M_{ii} \geq \sum_{j \mid j \neq i} \left| \frac{s_i M_{ij}^t}{s_j} \right| + \rho, \quad \forall i; \quad \sum_i M_{ii} \leq C. \end{aligned} \quad (31)$$

where $\text{vec}(\{M_{ii}\}) = [M_{1,1} \ M_{2,2} \ \dots \ M_{K,K}]^\top$ is a vector composed of diagonal terms $\{M_{ii}\}$, and M_{ij}^t are off-diagonal terms of previous solution \mathbf{M}^t . LP (31) can be solved efficiently using known fast algorithms such as Simplex [15] and interior point method [44].

4.4.2 FW Step 2: Step Size Optimization

The second FW step combines the newly computed solution $\{M_{ii}^o\}$ in step 1 with the previous solution $\{M_{ii}^t\}$ using step size γ , where $0 \leq \gamma \leq 1$:

$$M_{ii}^{t+1} = M_{ii}^t + \gamma(M_{ii}^o - M_{ii}^t), \quad \forall i \quad (32)$$

We compute the optimal step size γ as follows. Define *direction* $\{d_{ii}\}$ where $d_{ii} = M_{ii}^o - M_{ii}^t$. We solve a one-dimensional optimization problem for step size γ :

$$\min_{\gamma \mid 0 \leq \gamma \leq 1} Q(\mathbf{M}^t + \gamma \text{diag}(\{d_{ii}\})) \quad (33)$$

where $\text{diag}(\{d_{ii}\})$ is a diagonal matrix with $\{d_{ii}\}$ along its diagonal entries. Define $\mathbf{M}^* = \mathbf{M}^t + \gamma \text{diag}(\{d_{ii}\})$. Using the chain rule for multivariate functions, we write:

$$\frac{\partial Q(\mathbf{M}^*)}{\partial \gamma} = \sum_{i=1}^K \frac{\partial Q(\mathbf{M}^*)}{\partial M_{ii}^*} \frac{\partial M_{ii}^*}{\partial \gamma} \quad (34)$$

$$= \sum_{i=1}^K \frac{\partial Q(\mathbf{M}^*)}{\partial M_{ii}^*} d_{ii}. \quad (35)$$

Substituting $M_{ii}^* = M_{ii}^t + \gamma d_{ii}$ into (35), we can write $Q'(\gamma) = \frac{\partial Q(\mathbf{M}^*)}{\partial \gamma}$ as a function of γ only.

Since $Q(\mathbf{M})$ is convex, one-dimensional $Q(\gamma)$ is also convex, and $Q'(\gamma^*) = 0$ at a unique γ^* . In general, we cannot find γ^* in closed form given an arbitrary $Q(\mathbf{M})$. However, one can approximate γ^* quickly given derived $Q'(\gamma)$ using any root-finding algorithms, such as the Newton-Raphson (NR) method [45]. Given the range restriction of γ in (33), our proposed procedure to find step size γ^t at iteration t is thus the following:

- 1) Derive $Q'(\gamma)$ using (35) and compute minimizing γ^* using NR. If $Q'(\gamma)$ is a constant, then γ^* is either 0 or 1, depending on the sign of $Q'(\gamma)$.
- 2) Compute appropriate step size γ^t as follows:

$$\gamma^t = \begin{cases} 1 & \text{if } \gamma^* > 1 \\ 0 & \text{if } \gamma^* < 0 \\ \gamma^* & \text{o.w.} \end{cases} \quad (36)$$

The updated solution from FW iteration is then $\mathbf{M}^{t+1} = \mathbf{M}^t + \gamma^t \text{diag}(\{d_{ii}\})$. FW step 1 and 2 are executed repeatedly until convergence.

4.4.3 Comparing Frank-Wolfe and Proximal Gradient

After replacing the PD cone constraint with a series of linear constraints per iteration—thus defining a (more restricted) convex feasible space \mathcal{S} that is a polytope—one can conceivably use proximal gradient (PG) [6] instead of FW to optimize $Q(\mathbf{M})$. PG alternately performs a gradient descent step followed by a proximal operator that is a projection back to \mathcal{S} until convergence [46]. First, FW is entirely projection-free, while PG requires one convex set projection per iteration. More importantly, it is difficult in general to determine an optimal step size for gradient descent in PG—one that makes the maximal progress without overshooting. In the literature [6], PG step size can be determined based on Lipschitz

constant of $\nabla Q(\mathbf{M})$, which is expensive to compute if the Hessian matrix $\nabla^2 Q(\mathbf{M})$ is large. In contrast for FW, after direction $\{d_{ii}\}$ is determined in step 1, the objective $Q(\gamma)$ becomes one-dimensional, and thus optimal step size γ can be identified speedily using first- and second-order information $Q'(\gamma)$ and $Q''(\gamma)$. In our experiments, we show that our proposed FW-based optimization is faster than a previous PG-based method [46].

5 OPTIMIZING METRIC OFF-DIAGONALS

Including off-diagonal terms of metric \mathbf{M} into the optimization is more complicated, since modification of these terms may affect the balance and connectivity of the underlying graph. We design a block coordinate descent algorithm, which optimizes one row/column of off-diagonal terms *plus* diagonal terms at a time while maintaining graph balance.

5.1 Problem Formulation

First, we divide \mathbf{M} into four sub-matrices:

$$\mathbf{M} = \begin{bmatrix} M_{1,1} & \mathbf{M}_{2,1}^\top \\ \mathbf{M}_{2,1} & M_{2,2} \end{bmatrix}, \quad (37)$$

where $M_{1,1} \in \mathbb{R}$, $\mathbf{M}_{2,1} \in \mathbb{R}^{(K-1) \times 1}$ and $M_{2,2} \in \mathbb{R}^{(K-1) \times (K-1)}$. We optimize $\mathbf{M}_{2,1}$ and $\{M_{ii}\}$ in one iteration, *i.e.*,

$$\min_{\mathbf{M}_{2,1}, \{M_{ii}\}} Q(\mathbf{M}), \quad \text{s.t.} \quad \begin{cases} \mathbf{M} \succ 0 \\ \mathbf{M} \in \mathcal{S} \\ \sum_i M_{ii} \leq C \end{cases} \quad (38)$$

In the next iteration, a different node is selected, and with appropriate row/column permutation, we still optimize the first column off-diagonals $\mathbf{M}_{2,1}$ as in (38). For \mathbf{M} to remain a graph metric, i) \mathbf{M} must be PD, ii) \mathbf{M} must be balanced, and iii) \mathbf{M} must be irreducible.

5.2 Maintaining Graph Balance

We maintain graph balance during off-diagonal optimization as follows. Assuming graph \mathcal{G} from previous solution \mathbf{M}^t is balanced, nodes \mathcal{N} can be colored into blue nodes \mathcal{N}_b and red nodes \mathcal{N}_r . Suppose now node 1 is a blue node. Then we constrain edge weights to other blue/red nodes to be positive/negative. Combining these sign constraints with previously discussed GDA linear constraints to replace the PD cone constraint, the optimization becomes:

$$\min_{\mathbf{M}_{2,1}, \{M_{ii}\}} Q(\mathbf{M}), \quad \text{s.t.} \quad \begin{cases} M_{i,i}^t \geq \sum_{j \mid j \neq i} \left| \frac{s_i^t M_{i,j}}{s_j^t} \right| + \rho, \quad \forall i \\ M_{i,1} \leq 0, \quad \text{if } i \in \mathcal{N}_b \\ M_{i,1} \geq 0, \quad \text{if } i \in \mathcal{N}_r \\ \sum_i M_{ii} \leq C \end{cases} \quad (39)$$

Note that the sign for each $s_i^t M_{i,j} / s_j^t$ is known, given we know the scalar values s_i^t as well as the sign of $M_{i,j}$. Thus the absolute value operator can be appropriately removed, and the set of constraints remain linear.

Suppose instead that node 1 is a red node. Then the two edge sign constraints in (39) are replaced by

$$\begin{aligned} M_{i,1} &\geq 0, \quad \text{if } i \in \mathcal{N}_b \\ M_{i,1} &\leq 0, \quad \text{if } i \in \mathcal{N}_r \end{aligned}$$

After optimizing $\mathbf{M}_{2,1}$ twice, each time assuming node 1 is blue/red, we retain the better solution $\mathbf{M}_{2,1}^*$ that yields the smaller objective $Q(\mathbf{M})$. As an example, in Fig. 3 node 1's edges to other nodes are optimized assuming it is blue/red in the left/right graph. In both cases, the signs of the edge weights are constrained so that the graphs remain balanced.

(39) also has a convex differentiable objective with a set of linear constraints. We thus employ the aforementioned FW method to compute a solution. We omit the details for brevity.

5.3 Disconnected Sub-Graphs

The previous optimization assumes that the underlying graph \mathcal{G} corresponding to the generalized graph Laplacian \mathbf{M} is irreducible. When optimizing off-diagonal terms in \mathbf{M} also, \mathcal{G} may become disconnected into P separate sub-graphs $\mathcal{G}_1, \dots, \mathcal{G}_P$, with corresponding generalized graph Laplacian matrices $\mathbf{M}_1, \dots, \mathbf{M}_P$, where $\mathbf{M} = \text{diag}(\mathbf{M}_1, \dots, \mathbf{M}_P)$, *i.e.*, \mathbf{M} is block-diagonal. In this case, to compute scalars s_i in (29), we simply compute the first eigenvector \mathbf{v}_p via LOBPCG for each sub-matrix \mathbf{M}_p to derive scalars s_i for diagonals M_{ii} in \mathbf{M}_p . Optimization (39) can then be solved using the same FW method as described previously.

Given data $\mathbf{X} = [\mathbf{f}_1, \dots, \mathbf{f}_N]$, odd nodes being \mathcal{N}_b , even nodes being \mathcal{N}_r , and subgraph set \mathcal{G} , we summarize our optimization framework called *signed graph metric learning* (SGML) in Algorithm 1.

Algorithm 1 Signed Graph Metric Learning (SGML).

Input: $\mathbf{X}, C = K, \mathbf{M}^0 \succ 0, \mathcal{N}_b, \mathcal{N}_r, \mathcal{G}, \rho = 10^{-5}$.

Output: \mathbf{M}^* .

```

1: Compute scalars  $\{s^t\}$  via LOBPCG.
2: for  $i = 1 : K$ 
3:   while not converged do
4:     Solve (31) (w.r.t.  $\mathbf{M}_{2,1}, \{M_{ii}\}$ ).
5:     while not converged do
6:       Solve (33).
7:     end while
8:   end while
9: Do 3-8 with  $i \in \mathcal{N}_b, i \in \mathcal{N}_r$ , respectively, and choose
   solution with smaller objective.
10: Update  $\mathcal{G}$  if Node  $i$  is disconnected.
11: Update  $\{s^t\}$  via LOBPCG,  $\mathcal{N}_b$ , and  $\mathcal{N}_r$ .
12: end for
13: while not converged do
14:   Solve (31) (w.r.t.  $\mathbf{M}$ ).
15:   while not converged do
16:     Solve (33).
17:   end while
18: end while
19: return  $\mathbf{M}^*$ .

```

6 EXPERIMENTS

We evaluated our proposed SGML optimization in terms of: 1) computed objective values for different convex and differentiable objectives $Q(\mathbf{M})$'s against competing optimization schemes, 2) running time, and 3) performance in a specific application, namely binary classification, against competing metric learning schemes.

6.1 Objective Value and Running Time

We first compared computed objective values using SGML against two competing optimization schemes: 1) standard gradient descent with projection onto a PD cone for full \mathbf{M} optimization, and 2) a recent metric learning scheme using block coordinate descent with PG that adopts restricted search spaces that are intersections of half spaces, boxes and norm balls (HBNB) [46].

We evaluated PD-cone, HBNB, and SGML on the following $Q(\mathbf{M})$'s (also in Table 1) that 1) are convex and (partially) differentiable, and 2) require \mathbf{M} to be PD:

- 1) Maximally collapsing metric learning (MCML) [31].
- 2) Seminal distance metric learning (DEML) [4]. For the sake of comparison without losing validity of the optimization results, we relax the constraint $\sum_{\mathbf{f}_i, \mathbf{f}_j \in \mathcal{S}} \Delta \mathbf{f}_{ij}^\top \mathbf{M} \Delta \mathbf{f}_{ij} \leq c, c > 0$ (\mathcal{S} denotes the set of sample pairs that have the same labels) since solving this constrained problem (solving a sparse system of linear equations) may result in \mathbf{M} not being PD. See [4] for details.
- 3) Least squared-residual metric learning (LSML) [47]. We set the distance weights to be all 1's and no prior metric matrix is given.
- 4) Large margin nearest neighbor (LMNN) [1]. Note that the objective function is piecewise linear.
- 5) Graph Laplacian regularizer (GLR) [37], [48]:

$$\sum_{i=1}^N \sum_{j=1}^N \exp \{-(\mathbf{f}_i - \mathbf{f}_j)^\top \mathbf{M} (\mathbf{f}_i - \mathbf{f}_j)\} (z_i - z_j)^2. \quad (40)$$

A small GLR means that signal \mathbf{z} at connected node pairs (z_i, z_j) are similar for a large edge weight $w_{i,j}$, i.e., \mathbf{z} is *smooth* with respect to the variation operator $\sum_{i,j} \exp \{-(\mathbf{f}_i - \mathbf{f}_j)^\top \mathbf{M} (\mathbf{f}_i - \mathbf{f}_j)\}$.

We evaluated PD-cone, HBNB, and SGML using the 14 datasets in [49], *Sonar* with 60 features, *Madelon* with 500 features, and *Colon-cancer* with 2000 features, all of which are binary datasets available in UCI⁴ and LibSVM⁵. For each of the three above optimization schemes, we randomly split (with random seed 0) a dataset into $T = \text{round}(N/4)$ folds, ran optimization on each fold and took the average of the converged objective values. We ran similar experiments on datasets *Madelon* and *Colon-cancer*, except that we only ran the first 10 of T folds of the data and took the average. We applied the same data normalization scheme in [49] that 1) subtracts

the mean and divides by the standard deviation feature-wise, and 2) normalizes to unit length sample-wise. We added 10^{-12} noise to the dataset to avoid NaN's due to data normalization on small samples.

The parameters of PD-cone, HBNB and SGML are listed in Table 2. Finding a step size for PG based on Lipschitz constant for *Madelon* and *Colon-cancer* is computationally infeasible in a consumer-level machine, where Hessian $\nabla^2 Q(\mathbf{M})$'s have 500^4 and 2000^4 entries, respectively. Thus, as done in [1], the step size of gradient descent (GD) for PD-cone and HBNB was heuristically initialized as $0.1/N$, increased by 1% if GD yielded a better objective value, and decreased by half otherwise. For SGML, we solved LP's using Matlab linprog in Step 4 of Algorithm 1 and Gurobi Matlab interface⁶ in Step 14, both of which adopt interior-point.

The converged objective values in Table 3 and 4 show that, SGML achieved very close objective values to PD-cone, which is a high-complexity optimal scheme. SGML also consistently achieved larger objective values than HBNB in DEML maximization, and generally achieved smaller objective values than HBNB in MCML and GLR minimization. LSML minimization objective contains boolean expressions and LMNN minimization objective is piecewise linear, and thus they are not differentiable everywhere; SGML achieved comparable objective values to HBNB in these two cases. The search spaces defined in HBNB are generally too restrictive, resulting in sub-optimal solutions for many objectives.

All three optimization schemes were implemented in Matlab⁷. Fig. 4 and 5 show the total running time, as well as the most time-consuming components of PD-cone, HBNB, and SGML, on datasets *Madelon* and *Colon-cancer*. Both figures show that 1) eigen-decomposition for PD-cone on large matrices entailed high computation complexity, 2) it often took large numbers of iterations for PD-cone and HBNB to converge using a heuristic gradient descent step size selection (see Table 2), 3) SGML/HBNB benefited from LOBPCG for fast first eigenpair computation, and 4) SGML in addition benefited from the typical sparsity of computed \mathbf{M} ($a \ll K^2$ for LOBPCG complexity $\mathcal{O}(ab)$) and FW step size optimization, and thus converged much faster than PD-cone and HBNB. In particular, SGML was roughly 5x and 4x faster than PD-cone on *Madelon* with MCML and GLR objectives, respectively, as shown in Fig. 4, and 2x faster than PD-cone on *Colon-cancer* with MCML, DEML and GLR objectives, as shown in Fig. 5.

6.2 Binary Classification

Further, we evaluated SGML on binary classification using the same 14 binary datasets used in [49]. Since tailoring an algorithm to a specific objective function or

4. <https://archive.ics.uci.edu/ml/datasets.php>

5. <https://www.csie.ntu.edu.tw/~cjlin/libsvmtools/datasets/binary.html>

6. https://www.gurobi.com/documentation/9.0/examples/linprog_m.html

7. code available: <https://github.com/bobchengyang/SGML>

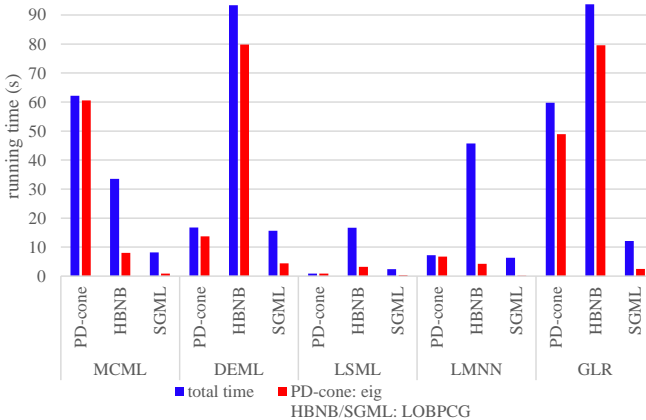


Fig. 4. Running time on *Madelon* of optimization methods PD-cone, HBNB, and SGML on various objective functions MCML, DEML, LSML, LMNN and GLR.

classifier is outside the scope of this paper, we heuristically evaluated our SGML algorithm on a GLR objective function and the following three classifiers:

- 1) 3-nearest neighbor implemented by authors of Information-Theoretic Metric Learning⁸ (ITML).
- 2) Mahalanobis⁹. The predicted class of sample f is the one that yields a smaller Mahalanobis distance: $\sqrt{(f - \mu_i)^\top M(f - \mu_i)}$, $i \in \{1, -1\}$, where μ_i denotes the mean value of each feature in one class of the training data.
- 3) Graph-based binary classifier. We first solve (40) via SGML for M given a label vector z with 100% known (fixed) labels. Then we re-define z that consists of both the known and unknown labels, and solve (40) as a QP via CVX for z given M .

As done in [49], we randomly (with random seeds 0-9) split each dataset into 60% training and 40% test sets, and took the average and standard deviation of accuracy of 10 runs. We compared SGML against the best 9 out of 13 metric learning algorithms tested in [49], in terms of the average classification accuracy of all 14 tested datasets. Table 5 shows that, using a GLR objective, SGML on three classifiers achieved the best classification results in 7 out of 14 datasets and remained competitive (within 3%) for 12 out of 14 datasets. This may be due to the fact that GLR promotes smoothness within each piece of the binary label signal and the difference at the boundary of the two pieces of the label signal.

7 CONCLUSION

A fundamental challenge in metric learning is to efficiently handle the constraint of metric matrix M inside the positive definite (PD) cone. Circumventing full eigen-decomposition, we propose a fast, general optimization

8. <http://www.cs.utexas.edu/users/pjain/itml/download/itml-1.2.tar.gz>

9. https://github.com/LEMINHDONG161/BSS-Euclidean_Mahalanobis_Bayes_Classifier/blob/master/mahalanobis_classifier.m

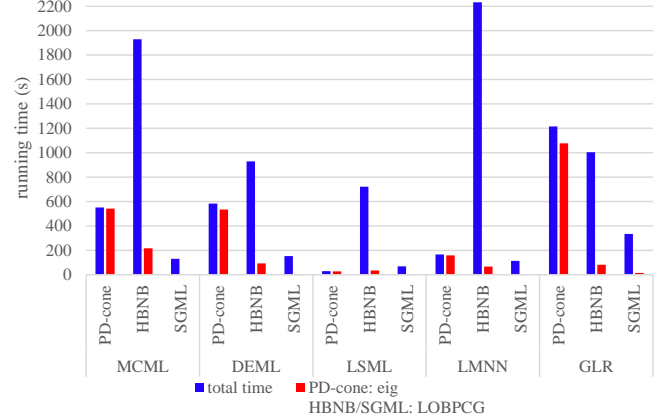


Fig. 5. Running time on *Colon-cancer* of optimization methods PD-cone, HBNB, and SGML on various objective functions MCML, DEML, LSML, LMNN and GLR.

framework capable of minimizing any convex and differentiable objective $Q(M)$. The theoretical foundation is Gershgorin disc alignment (GDA): all Gershgorin disc left-ends of a generalized graph Laplacian matrix corresponding to an irreducible, balanced signed graph can be perfectly aligned via a similarity transform. This enables us to write tightest possible linear constraints per iteration to replace the PD cone constraint, allowing us to solve the optimization as linear programs via the Frank-Wolfe method. We envision that GDA can also be used in other optimization problems with PD / PSD cone constraints, such as semi-definite programs (SDP).

REFERENCES

- [1] K. Q. Weinberger and L. K. Saul, "Distance metric learning for large margin nearest neighbor classification," *Journal of Machine Learning Research*, vol. 10, no. 2, pp. 207–244, Feb. 2009.
- [2] P. C. Mahalanobis, "On the generalized distance in statistics," *Proceedings of the National Institute of Sciences of India*, vol. 2, no. 1, pp. 49–55, April 1936.
- [3] M. Vetterli, J. Kovacevic, and V. Goyal, *Foundations of Signal Processing*. Cambridge University Press, 2014.
- [4] E. P. Xing, M. I. Jordan, S. J. Russell, and A. Y. Ng, "Distance metric learning with application to clustering with side-information," in *NIPS*, Dec. 2003, pp. 521–528.
- [5] J. V. Davis, B. Kulis, P. Jain, S. Sra, and I. S. Dhillon, "Information-theoretic metric learning," in *ICML*, 2007, pp. 209–216.
- [6] N. Parikh and S. Boyd, "Proximal algorithms," *Foundations and Trends in Optimization*, vol. 1, no. 3, pp. 127–239, Jan. 2014.
- [7] G.-J. Qi, J. Tang, Z.-J. Zha, T.-S. Chua, and H.-J. Zhang, "An efficient sparse metric learning in high-dimensional space via l_1 -penalized log-determinant regularization," in *ICML*, June 2009, pp. 841–848.
- [8] D. Lim, G. Lanckriet, and B. McFee, "Robust structural metric learning," in *ICML*, June 2013, pp. 615–623.
- [9] W. Liu, C. Mu, R. Ji, S. Ma, J. R. Smith, and S.-F. Chang, "Low-rank similarity metric learning in high dimensions," in *AAAI*, Jan. 2015, p. 27922799.
- [10] Y. Mu, "Fixed-rank supervised metric learning on Riemannian manifold," in *AAAI*, Feb. 2016, pp. 1941–1947.
- [11] J. Zhang and L. Zhang, "Efficient stochastic optimization for low-rank distance metric learning," in *AAAI*, Feb. 2017, pp. 933–939.
- [12] C. Yang, G. Cheung, and V. Stankovic, "Alternating binary classifier and graph learning from partial labels," in *APSIPA*, Nov. 2018, pp. 1137–1140.

TABLE 1
Tested convex and (partially) differentiable objective functions $Q(\mathbf{M})$'s. $d_{\mathbf{M}}(i, j) = \Delta \mathbf{f}_{ij}^\top \mathbf{M} \Delta \mathbf{f}_{ij}$.

	MCML	DEML	LSML	LMNN	GLR
$Q(\mathbf{M})$	$\sum_{i,j: y_j = y_i} d_{\mathbf{M}}(i, j) + \sum_i \log \sum_{k \neq i} \exp \{-d_{\mathbf{M}}(i, k)\}$	$\sum_{\mathbf{f}_i, \mathbf{f}_j \in \mathcal{D}} \sqrt{d_{\mathbf{M}}(i, j)}$	$\sqrt{d_{\mathbf{M}}(a, b)} > \sqrt{d_{\mathbf{M}}(c, d)} \sum_{\mathbf{f}_a, \mathbf{f}_b \in \mathcal{S}, \mathbf{f}_c, \mathbf{f}_d \in \mathcal{D}} \left(\sqrt{d_{\mathbf{M}}(a, b)} - \sqrt{d_{\mathbf{M}}(c, d)} \right)^2$	$(1 - \mu) \sum_{i,j \sim i} d_{\mathbf{M}}(i, j) + \mu \sum_{i,j \sim i} \sum_l (1 - y_{il}) \left[1 + d_{\mathbf{M}}(i, j) - d_{\mathbf{M}}(i, l) \right]_+$	$\sum_{i,j} \exp \{-d_{\mathbf{M}}(i, j)\} (z_i - z_j)^2$

TABLE 2
Optimization parameters. GD=gradient descent.

Parameters	PD-cone	HBNN	SGML
main tol		1.00E-05	
max main iter.		1.00E+03	
GD step size	$t_0 = 0.1/N$ $t_k = 1.01t_{k-1}$, if GD yields better obj. $t_k = t_{k-1}/2$, o.w.[1]	-	-
dia/offdia tol		1.00E-03	
max dia/offdia/FW iter.	-	1.00E+03	
LOBPCG tol		1.00E-04	
max LOBPCG iter.		2.00E+02	
LP optimality tol		1.00E-02	
LP interior-point tol		1.00E-04	
Frank-Wolfe step size		NR with 0.5 tol	

- [13] T. Biyikoglu, J. Leydold, and P. F. Stadler, "Nodal domain theorems and bipartite subgraphs," *The Electronic Journal of Linear Algebra*, vol. 13, pp. 344–351, Jan. 2005.
- [14] R. S. Varga, *Gershgorin and his circles*. Springer, 2004.
- [15] C. Papadimitriou and K. Steiglitz, *Combinatorial Optimization*. Dover Publications, Inc, 1998.
- [16] M. Jaggi, "Revisiting Frank-Wolfe: Projection-free sparse convex optimization," in *ICML*, Jun 2013, pp. 427–435.
- [17] A. V. Knyazev, "Toward the optimal preconditioned eigen-solver: Locally optimal block preconditioned conjugate gradient method," *SIAM Journal on Scientific Computing*, vol. 23, no. 2, pp. 517–541, 2001.
- [18] G. Tsagkatakis and A. Savakis, "Manifold modeling with learned distance in random projection space for face recognition," in *ICPR*. IEEE, 2010, pp. 653–656.
- [19] M. Schultz and T. Joachims, "Learning a distance metric from relative comparisons," in *NIPS*, 2004, pp. 41–48.
- [20] L. Torresani and K.-c. Lee, "Large margin component analysis," in *NIPS*, 2007, pp. 1385–1392.
- [21] S. Mika, G. Ratsch, J. Weston, B. Scholkopf, and K.-R. Mullers, "Fisher discriminant analysis with kernels," in *Neural networks for signal processing IX: Proceedings of the 1999 IEEE signal processing society workshop (cat. no. 98th8468)*, 1999, pp. 41–48.
- [22] J. Lu, J. Hu, and J. Zhou, "Deep metric learning for visual understanding: An overview of recent advances," *IEEE Signal Processing Magazine*, vol. 34, no. 6, pp. 76–84, 2017.
- [23] R. Hadsell, S. Chopra, and Y. LeCun, "Dimensionality reduction by learning an invariant mapping," in *IEEE CVPR*, vol. 2, 2006, pp. 1735–1742.
- [24] Y. Taigman, M. Yang, M. Ranzato, and L. Wolf, "Deepface: Closing the gap to human-level performance in face verification," in *IEEE CVPR*, 2014, pp. 1701–1708.
- [25] J. Hu, J. Lu, and Y.-P. Tan, "Discriminative deep metric learning for face verification in the wild," in *IEEE CVPR*, 2014, pp. 1875–1882.
- [26] Y. Sun, Y. Chen, X. Wang, and X. Tang, "Deep learning face representation by joint identification-verification," in *Advances in neural information processing systems*, 2014, pp. 1988–1996.
- [27] J. Wang, Y. Song, T. Leung, C. Rosenberg, J. Wang, J. Philbin, B. Chen, and Y. Wu, "Learning fine-grained image similarity with deep ranking," in *IEEE CVPR*, 2014, pp. 1386–1393.
- [28] E. Hoffer and N. Ailon, "Deep metric learning using triplet network," in *International Workshop on Similarity-Based Pattern Recognition*. Springer, 2015, pp. 84–92.
- [29] F. Schroff, D. Kalenichenko, and J. Philbin, "Facenet: A unified

- embedding for face recognition and clustering," in *IEEE CVPR*, 2015, pp. 815–823.
- [30] H. Oh Song, Y. Xiang, S. Jegelka, and S. Savarese, "Deep metric learning via lifted structured feature embedding," in *IEEE CVPR*, 2016, pp. 4004–4012.
- [31] A. Globerson and S. T. Roweis, "Metric learning by collapsing classes," in *NIPS*, 2006, pp. 451–458.
- [32] Y. Ying and P. Li, "Distance metric learning with eigenvalue optimization," *JMLR*, vol. 13, no. Jan, pp. 1–26, 2012.
- [33] P. Zadeh, R. Hosseini, and S. Sra, "Geometric mean metric learning," in *ICML*, June 2016, pp. 2464–2471.
- [34] Y. Bai, G. Cheung, F. Wang, X. Liu, and W. Gao, "Reconstruction-cognizant graph sampling using Gershgorin disc alignment," in *ICASSP*, May 2019, pp. 5396–5400.
- [35] Y. Bai, F. Wang, G. Cheung, Y. Nakatsukasa, and W. Gao, "Fast graph sampling set selection using Gershgorin disc alignment," *IEEE Transactions on Signal Processing*, March 2020.
- [36] C. Yang, G. Cheung, and W. Hu, "Fast graph metric learning via Gershgorin disc alignment," in *IEEE ICASSP*, May 2020.
- [37] A. Ortega, P. Frossard, J. Kovaevi, J. M. F. Moura, and P. Vandergheynst, "Graph signal processing: Overview, challenges, and applications," *Proc. IEEE*, vol. 106, no. 5, pp. 808–828, May 2018.
- [38] M. Milgram, "Irreducible graphs," *Journal Of Combinatorial Theory (B)*, vol. 12, pp. 6–31, Feb. 1972.
- [39] G. Cheung, E. Magli, Y. Tanaka, and M. K. Ng, "Graph spectral image processing," *Proc. IEEE*, vol. 106, no. 5, pp. 907–930, 2018.
- [40] G. H. Golub and C. F. Van Loan, *Matrix Computations*, 3rd ed. The Johns Hopkins University Press, 1996.
- [41] R. Horn and C. Johnson, *Matrix Analysis*. Cambridge University Press, 2012.
- [42] D. Cartwright and F. Harary, "Structural balance: a generalization of heider's theory," *Psychological Review*, vol. 63, no. 5, pp. 277–293, 1956.
- [43] J. Leskovec, D. Huttenlocher, and J. Kleinberg, "Signed networks in social media," in *SIGCHI Conference on Human Factors in Computing Systems*, April 2010, p. 13611370.
- [44] S. Boyd and L. Vandenberghe, *Convex Optimization*. Cambridge University Press, 2009.
- [45] J. Raphson, *Analysis aequationum universalis*, London, 1690.
- [46] W. Hu, X. Gao, G. Cheung, and Z. Guo, "Feature graph learning for 3D point cloud denoising," *IEEE TSP*, vol. 68, pp. 2841–2856, 2020.
- [47] E. Y. Liu, Z. Guo, X. Zhang, V. Jojic, and W. Wang, "Metric learning from relative comparisons by minimizing squared residual," in *IEEE ICDM*, Dec. 2012, pp. 978–983.
- [48] J. Pang and G. Cheung, "Graph Laplacian regularization for image denoising: Analysis in the continuous domain," *IEEE TIP*, vol. 26, no. 4, pp. 1770–1785, April 2017.
- [49] M. Dong, Y. Wang, X. Yang, and J. Xue, "Learning local metrics and influential regions for classification," *IEEE TPAMI*, vol. 42, no. 6, pp. 1522–1529, June 2020.
- [50] M. Perrot and A. Habrard, "Regressive virtual metric learning," in *NIPS*, Dec. 2015, pp. 1810–1818.
- [51] J. Wang, A. Kalousis, and A. Woznica, "Parametric local metric learning for nearest neighbor classification," in *Advances in Neural Information Processing Systems 25*, Dec. 2012, pp. 1601–1609.
- [52] B. Nguyen, C. Morell, and B. D. Baets, "Supervised distance metric learning through maximization of the jeffrey divergence," *Pattern Recognition*, vol. 64, pp. 215 – 225, April 2017.
- [53] Y. Shi, A. Bellet, and F. Sha, "Sparse compositional metric learning," in *AAAI*, July 2014, p. 20782084.
- [54] Y. Huang, C. Li, M. Georgopoulos, and G. C. Anagnostopoulos, "Reduced-rank local distance metric learning," in *Machine Learning and Knowledge Discovery in Databases*, Sept. 2013, pp. 224–239.

TABLE 3

Converged objective values. All problems minimize $Q(\mathbf{M})$'s except DEML. The better objective values between HBNB and SGML are in bold. (avg. of $T = \text{round}(N/4)$ runs; data is split into T folds and run T times; timed experiments on *madelon* and *colon-cancer* are run on the first 10 out of T folds and then take the avg.; \mathbf{M} initialized as diagonal entries being equal to 1 and first off-diagonal entries being equal to 0.1; machine spec: Intel Core i7-9700K 3.60GHz Windows 10 64bit 32GB of RAM)

$Q(\mathbf{M})$	dataset (N, K)	Australian (690,14)	Breastcancer (683,10)	Diabetes (768,8)	Fourclass (862,2)	German (1000,24)	Haberman (206,3)	Heart (270,13)	ILPD (583,10)
MCML	PD-cone	5.21E-03	1.17E-02	3.46E-02	9.11E-01	1.12E-02	2.86E-01	2.80E-03	3.78E-02
	HBNB	3.54E-01	9.37E-02	5.79E-01	1.07E+00	2.13E-01	4.77E-01	3.57E-01	2.86E-01
	SGML	1.74E-01	4.26E-02	4.27E-01	1.00E+00	9.71E-02	4.14E-01	1.37E-01	2.23E-01
DEML	PD-cone	1.62E+01	1.75E+01	1.16E+01	6.63E+00	1.80E+01	6.47E+00	1.57E+01	1.14E+01
	HBNB	8.81E+00	9.06E+00	8.09E+00	6.87E+00	7.56E+00	6.26E+00	8.80E+00	7.27E+00
	SGML	1.01E+01	1.01E+01	8.97E+00	6.95E+00	9.32E+00	6.57E+00	9.99E+00	8.33E+00
LSML	PD-cone	8.56E-03	1.25E-03	5.68E-03	4.73E-01	1.71E-02	7.54E-02	7.57E-03	1.43E-02
	HBNB	2.32E-02	1.03E-03	2.40E-02	5.20E-01	3.27E-02	1.24E-01	1.49E-02	6.09E-02
	SGML	3.54E-02	5.15E-04	7.88E-02	2.48E-02	1.16E-02	7.32E-02	2.21E-02	6.69E-02
LMNN	PD-cone	7.33E+00	6.72E+00	6.55E+00	8.64E+00	6.21E+00	6.49E+00	7.38E+00	6.12E+00
	HBNB	9.17E+00	8.10E+00	9.69E+00	9.45E+00	7.93E+00	8.62E+00	9.50E+00	8.54E+00
	SGML	9.94E+00	8.20E+00	9.57E+00	9.68E+00	8.69E+00	8.40E+00	1.00E+01	9.15E+00
GLR	PD-cone	3.50E-03	1.13E-03	3.79E-02	1.66E+00	1.04E-03	6.29E-01	1.34E-03	2.58E-02
	HBNB	1.63E-01	5.88E-02	2.28E-01	1.57E+00	1.28E-01	6.78E-01	1.36E-01	2.02E-01
	SGML	1.25E-01	2.55E-02	2.79E-01	1.61E+00	5.92E-02	6.96E-01	1.11E-01	1.48E-01

TABLE 4

Continuation of Table 3 on other datasets. The better objective values between HBNB and SGML are in bold. All problems minimize $Q(\mathbf{M})$'s except DEML.

$Q(\mathbf{M})$	dataset (N, K)	Liverdisorders (345,6)	Monk1 (556,6)	Pima (768,8)	Planning (182,12)	Voting (435,16)	WDBC (569,30)	Sonar (208,60)	madelon (2600,500)	colon-cancer (62,2000)
MCML	PD-cone	1.85E-01	1.12E-01	3.95E-02	3.52E-02	1.01E-02	9.34E-03	2.14E-03	9.95E-04	6.01E-03
	HBNB	8.96E-01	1.15E+00	5.41E-01	2.84E-01	1.07E-01	1.43E-01	4.36E-01	4.42E-01	4.50E-01
	SGML	6.55E-01	7.28E-01	4.35E-01	1.73E-01	2.04E-02	5.40E-02	1.23E-01	1.64E-02	3.83E-02
DEML	PD-cone	9.64E+00	1.04E+01	1.15E+01	1.24E+01	1.94E+01	2.68E+01	3.17E+01	8.92E+01	1.56E+02
	HBNB	8.04E+00	8.30E+00	8.00E+00	7.17E+00	9.04E+00	8.79E+00	8.46E+00	8.30E+00	6.83E+00
	SGML	8.56E+00	8.96E+00	8.79E+00	8.10E+00	1.05E+01	1.04E+01	1.08E+01	1.12E+01	9.28E+00
LSML	PD-cone	8.80E-03	3.23E-03	4.33E-03	5.07E-03	3.10E-03	2.09E-03	6.86E-03	2.34E-03	1.20E-02
	HBNB	6.08E-02	2.83E-02	2.63E-02	1.87E-02	9.27E-03	9.60E-03	1.71E-02	6.60E-03	3.50E-02
	SGML	1.32E-01	9.05E-02	7.48E-02	4.39E-02	9.76E-03	3.61E-03	4.72E-03	3.99E-06	2.96E-04
LMNN	PD-cone	6.89E+00	8.09E+00	6.59E+00	6.06E+00	6.97E+00	6.92E+00	8.20E+00	7.98E+00	6.50E+00
	HBNB	9.69E+00	1.06E+01	9.57E+00	8.14E+00	8.35E+00	8.36E+00	9.84E+00	1.04E+01	8.70E+00
	SGML	9.85E+00	1.05E+01	9.60E+00	8.58E+00	9.50E+00	9.53E+00	1.23E+01	1.11E+01	8.49E+00
GLR	PD-cone	2.15E-01	1.19E-01	4.08E-02	1.90E-03	1.15E-03	1.00E-03	1.00E-03	9.88E-04	9.75E-04
	HBNB	4.13E-01	3.70E-01	2.58E-01	1.61E-01	8.66E-02	9.45E-02	2.62E-01	2.28E-01	1.08E-01
	SGML	4.32E-01	5.04E-01	2.73E-01	1.21E-01	2.69E-02	3.65E-02	8.47E-02	8.80E-02	6.02E-02

TABLE 5

Classification accuracy of metric learning algorithms. avg. of 10 runs (random seeds 0-9). Results of competing schemes are copied from [49].

Datasets	RVML	PLML	mmLMNN	GMML	DMLMJ	SCML	DMLE	R2LML	LMLIR	SGML (prop.)		
	[50]	[51]	[1]	[33]	[52]	[53]	[32]	[54]	[49]	3-NN Mahalanobis Graph		
australian	83.0±1.6	80.5±1.1	82.5±2.6	84.4±1.0	83.9±1.3	82.3±1.4	82.6±1.5	84.7±1.3	85.1±1.9	83.3±1.2	84.8±1.3	85.3±1.7
breastcancer	95.8±1.1	96.4±0.9	96.7±1.0	97.3±0.8	96.6±0.8	97.0±0.9	97.0±1.1	97.0±0.7	96.4±2.1	97.6±1.0	98.0±0.6	97.6±0.7
diabetes	71.0±2.6	68.5±2.0	72.2±1.9	74.2±2.6	71.5±3.1	71.5±2.2	72.6±2.0	73.8±1.4	75.9±1.9	71.6±1.8	70.5±2.5	70.3±1.4
fourclass	70.5±1.4	72.4±2.4	75.6±1.4	76.1±1.9	76.1±1.9	75.5±1.4	75.6±1.4	76.1±1.9	79.9±0.9	74.5±2.4	71.1±1.6	78.0±1.2
german	71.7±1.8	70.0±2.9	68.9±1.8	71.6±1.1	69.3±2.7	70.9±2.7	72.0±2.1	72.9±1.8	73.7±1.6	71.6±1.7	70.9±1.3	70.0±0.0
haberman	66.7±2.3	67.1±3.1	69.0±2.7	71.2±3.4	68.5±3.2	69.2±2.5	70.8±3.5	71.1±3.4	74.4±3.7	68.8±3.9	66.6±6.3	73.6±0.3
heart	77.7±4.1	75.1±3.2	79.4±3.7	81.2±2.7	80.6±2.8	79.0±3.2	77.9±3.1	82.0±3.8	83.1±3.2	81.0±3.4	83.2±3.6	83.6±3.5
ILPD	68.0±2.9	67.4±3.0	66.8±2.1	67.1±2.2	68.0±1.6	68.0±2.9	68.8±2.7	65.9±2.2	69.6±2.7	65.2±2.4	59.1±2.4	71.3±0.2
liverdisorders	64.6±3.9	62.2±2.5	62.0±3.5	63.8±5.4	60.9±3.8	61.7±4.6	61.8±2.7	66.8±3.7	66.7±3.6	69.5±3.3	68.8±5.9	72.1±3.0
monk1	89.2±2.7	96.6±2.7	90.3±2.6	75.0±2.6	87.7±3.8	97.5±0.9	99.9±0.3	89.2±1.5	95.0±7.2	84.6±5.1	66.3±3.0	71.1±3.7
pima	69.5±1.7	68.4±2.2	72.5±2.7	73.0±1.8	71.1±2.8	71.1±2.6	72.1±2.4	72.3±1.5	74.6±2.0	73.4±1.3	73.6±2.0	69.2±1.5
planning	55.1±7.4	60.8±5.5	54.7±0.9	65.2±5.5	64.3±2.9	61.9±5.0	60.1±5.5	63.9±3.4	67.5±6.5	62.8±4.1	48.8±4.8	71.3±0.7
voting	95.8±1.3	95.5±1.0	95.4±0.9	95.2±1.9	95.3±1.1	95.0±1.3	93.1±1.9	96.3±1.2	93.2±3.9	96.4±1.4	94.3±2.0	94.8±1.6
WDBC	96.6±1.3	96.4±0.9	97.4±1.0	96.7±0.8	97.3±1.9	97.0±0.9	96.7±0.5	96.9±1.7	96.6±1.0	94.8±1.2	96.2±1.1	
Average	76.7	76.9	77.3	77.9	77.9	78.4	78.6	79.2	80.8	78.4	75.1	78.9
# of best	0	0	1	0	0	0	1	0	5	1	1	5